From Lithium to Uranium: Elemental Tracers of Early Cosmic Evolution
Proceedings IAU Symposium No. 228, 2005
V. Hill, P. François & F. Primas, eds.

doi:10.1017/S1743921305005430

Hierarchical growth and star formation: population III, reionization and nucleosynthesis

Frédéric Daigne and Elisabeth Vangioni

Institut d'Astrophysique de Paris, UMR 7095 CNRS, Université Pierre et Marie Curie,
98 bis boulevard Arago, 75014 Paris France
email: daigne,vangioni@iap.fr

Abstract.
Motivated by the WMAP results indicating an early epoch of reionization, we consider alternative cosmic star formation models which are capable of reionizing the early intergalactic medium. We develop models which include an early burst of massive stars (with several possible mass ranges) combined with standard star formation, in the framework of the hierarchical scenario of structure formation. We compute as a function of redshift the stellar ionizing flux of photons, the supernova rates and the chemical evolution, both in the intergalactic medium and in the interstellar medium of forming galaxies. We apply constraints from the cosmic observed star formation rate and the observed abundances in the Lyman α forest and in Damped Lyman α clouds in conjunction with the ability of the models to produce the required degree of reionization.

Keywords. Cosmology: theory, galaxies: evolution, Galaxy: evolution, nuclear reactions, nucleosynthesis, abundances, stars: evolution

---

1. Introduction

We have developed a model of cosmic evolution (Daigne *et al.* (2004), Daigne *et al.* (2005)), which is a generalized version of standard chemical evolution models designed to follow one specific structure such as the Milky Way (for a review, see Tinsley(1980)). We describe baryons in the Universe by two large reservoirs. The first one stands for the collapsed structures which form stars (hereafter the "structures") and is divided in two sub-reservoirs : the gas (hereafter the "interstellar medium" or ISM) and the stars and their remnants (hereafter the "stars"). The second reservoir stands for the medium lying between the collapsed structures (hereafter the "intergalactic medium" or IGM). We follow the evolution of the baryonic mass of these reservoirs as a function of redshift. It is governed by four mass fluxes, which represent four fundamental physical processes : structure formation (accretion of baryons from the IGM by the structures), star formation (transfer of baryons from the ISM to the stars), metal ejection by stars (transfer of baryons from the stars to the ISM) and enriched gas outflow from the structures (transfer of baryons from the ISM to the IGM). We follow not only the evolution of the baryonic mass of each reservoir but also the mass fraction of several chemical elements, the rate of explosive events (type Ia and type II supernovae) and the ionizing flux of stellar origin. The normal mode of star formation (0.1-100 $M_\odot$) dominates during most of the cosmic evolution. At high redshift and low metallicity, we consider a peculiar mode of star formation (population III stars) with a top-heavy IMF in the range 40-100 $M_\odot$. We have also considered very massive stars in the range 140-260 $M_\odot$ or in the range 270-500 $M_\odot$. The transition from population III stars to the normal mode of star formation occurs at

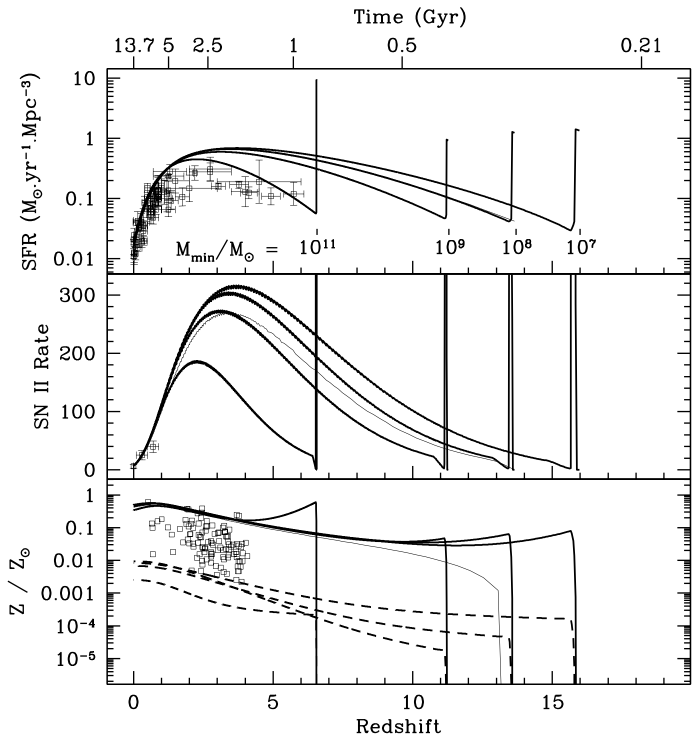

Figure 1. Cosmic star formation rate, type II supernova rate and global metallicity. *Top : Star formation rate as a function of redshift.* The observed SFR up to $z \sim 5$ is taken from Hopkins (2004). *Middle : Type II supernova rate as a function of redshift.* The observed rate up to $z \sim 0.7$ is taken from Dahlen *et al.* (2004). *Bottom : Global metallicity as a function of redshift.* The metallicity of 100 Damped Lyman-α systems measured by Prochaska *et al.* (2003) is indicated. In the three panels, the result of four models characterized by different minimum mass $M_{\rm min}$ of the dark matter halo of star-forming structures (see text) is plotted in thick line. Each value $M_{\rm min} = 10^7$, 10^8, 10^9 and 10^{11} $M_\odot$ is indicated in the upper panel and corresponds to a different initial redshift. In the lower panel, the solide line (resp. dashed line) represents the metallicity in the structures (resp. in the IGM). In each panel a model without outflow and without population III stars is also indicated in thin line for the case $M_{\rm min} = 10^8$ $M_\odot$.

a critical metallicity Z_c which is taken to be 10^{-4} $Z_\odot$ (Bromm (2004)). The structure formation is computed in the framework of the hierarchical scenario, using a code developed by Jenkins *et al.* (2001) based on the standard theory (Press & Schechter (1974)) which predicts the distribution of the mass of dark matter halos as a function of redshift. We use the cosmological parameters of the so-called "concordance model" (Spergel *et al.* (2003)). The growth of the reservoir of baryons in the structures is computed assuming that stars form in collapsed structures having a dark matter halo of minimum mass $M_{\rm min}$ and that this process starts when the fraction of baryons in such structures is 1 %. The outflow from the structures is assumed to be powered by a fraction ϵ of the kinetic energy of supernovae. The escape velocity in the structures evolves with redshift to take into account the increase of the typical mass of a star forming structure. Therefore the outflow is much more efficient at high redshift than today.

The model is therefore characterized by five physical parameters : minimum mass $M_{\rm min}$ of the dark matter halo of star-forming structures, efficiency ϵ of the outflow, slope x_1 of the IMF, intensity ν_1 and timescale τ_1 of the SFR, which decays exponentially with time

https://doi.org/10.1017/S1743921305005430 Published online by Cambridge University Press

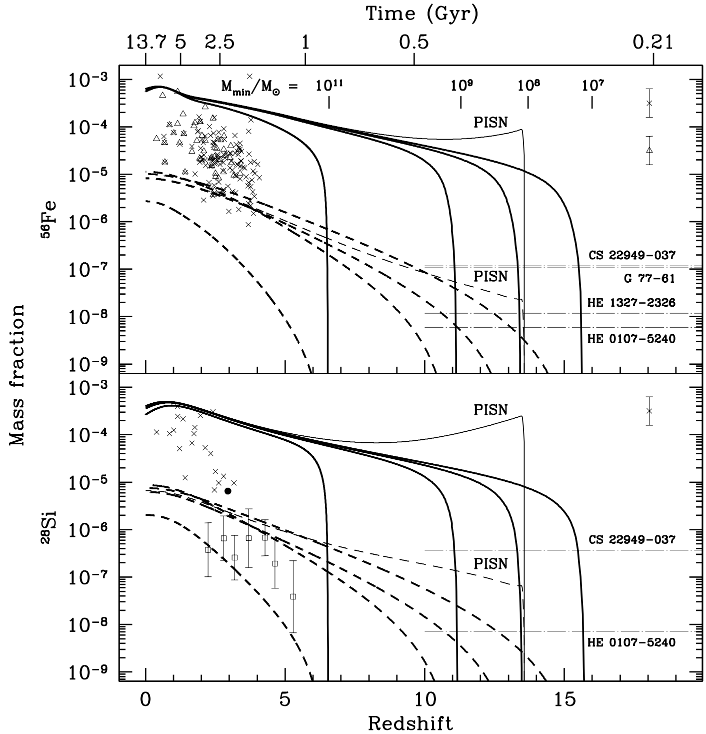

Figure 2. Evolution of the Iron and Silicon abundances. The mass fraction of Iron (top) and Silicon (bottom) as a function of redshift is plotted in thick line both in the ISM of structures (solid line) and in the IGM (dashed line) for four models characterized by $M_{\min} = 10^7$, 10^8, 10^9 and 10^{11} $M_\odot$. In the case $M_{\min} = 10^8$ $M_\odot$, an alternative model with very massive population III stars in the 140-260 $M_\odot$ mass range is also plotted in thin dashed line and labeled with PISN. Observed abundances are taken from Prochaska *et al.* (2003) (crosses: Iron and Silicon abundances in 100 DLAs), Ledoux *et al.* (2003) (triangles: Iron and Silicon abundances in 33 DLAs and sub-DLAs), Songaila (2001) (boxes: Silicon IV abundance in the IGM) and Aguirre *et al.* (2004) (big dot : total Silicon abundance in the IGM). Horizontal thin dashed lines indicate the measured abundances in the following four very metal-poor halo stars : CS 22949-037 (Iron and Silicon, from Depagne *et al.* (2002)), HE 0107-2240 (Iron and Silicon, from Bessell *et al.* (2004)), HE 1327-2326 (Iron, from Frebel *et al.* (2005) and G 77-61 (Iron, from Plez & Cohen (2005)).)

(for details see Daigne *et al.* (2005)). There are many observational constraints that can be used to fix these parameters : the observed cosmic star formation rate up to $z \sim 5$, the present value of the fraction of all baryons which are in the star-forming structures $f_{\rm b,struct}(z = 0) \sim 55 \pm 15$ % (Fukugita & Peebles (2004)), the observed rate of type II supernovae up to $z \sim 0.7$, the observed rate of type Ia supernovae up to $z \sim 1.6$ and the measurements of the abundances of several metals in the ISM and in the IGM up to $z \sim 5$.

2. Cosmic Star Formation Rate, reionization and nucleosynthesis

We build a series of models for different minimum mass $M_{\min}$ of the dark matter halo of star-forming structures. The timescale of the SFR is fixed to fit the observed SFR (shape of the decrease at low redshift), the intensity of the SFR is fixed by the observed

https://doi.org/10.1017/S1743921305005430 Published online by Cambridge University Press

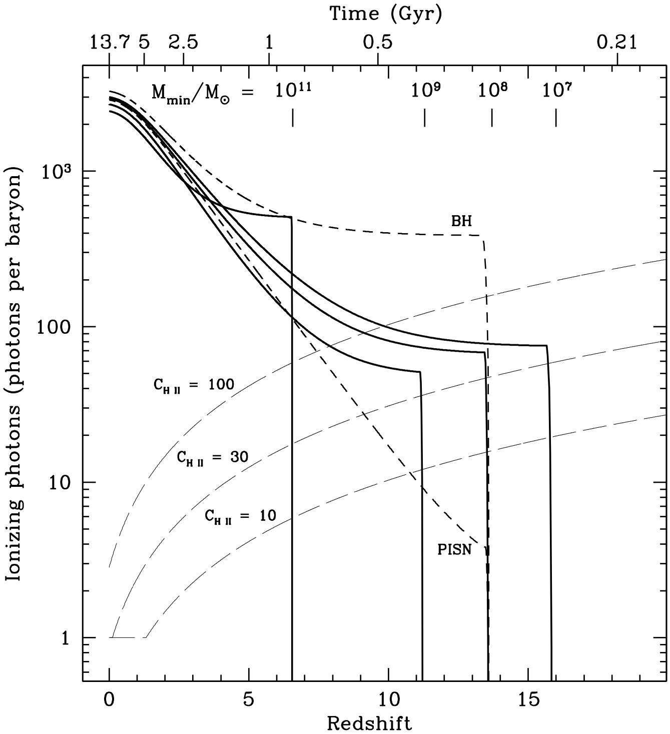

Figure 3. Reionization. The cumulative number of ionizing photons emitted by stars is plotted as a function of redshift for four different models characterized by $M_{\rm min} = 10^7$, 10^8, 10^9 and 10^{11} $M_\odot$. In the case $M_{\rm min} = 10^8$ $M_\odot$, two alternative models with very massive population III stars are also indicated in dahsed line. The model labeled PISN (resp. BH) corresponds to population III stars in the range 140-260 $M_\odot$ (resp. 270-500 $M_\odot$). These stars are assumed to end as a Pair-Instability Supernova (PISN) or to collapse directly into a black hole without any metal production (BH). The minimum number of photons per baryon necessary to fully reionize the IGM is plotted in thin dashed line for three different values of the clumpiness factor $C_{\rm H\ II} = 10$, 30 and 100.

metal abundances in the ISM, the efficiency of the outflow is adjusted to reproduce the observed present value of the baryon fraction in the star-forming structures and finally the slope of the IMF is fixed to fit the observed type II supernova rate. Once the normal mode is adjusted, a massive population III mode is added at high redshift for $Z < Z_{\rm c}$. The intensity of this early starburst is taken as large as possible to get a high ionizing flux at high redshift, under the constrain that one should avoid an overproduction of metals leading to a too intense prompt initial enrichment of the ISM and the IGM. Results for $M_{\rm min} = 10^7$, 10^8, 10^9 and 10^{11} $M_\odot$ are plotted in figures 1, 2 and 3. All these models give a present value of the baryon fraction in the structures in agreement with Fukugita & Peebles (2004) and reproduce well the observed SFR up to $z \sim 2-3$, the local global metallicity in the structures and the type II supernova rate up to $z \sim 0.7$. We find that the early enrichment of the IGM is easier at low minimum dark matter halo mass $M_{\rm min}$ (see figure 1 bottom), as the star formation starts earlier. This effect is even more visible for individual elements (see Iron and Silicon in figure 2). On the other hand the reionization of the IGM is less efficient for low $M_{\rm min}$ as the recombination time of ions is shorter at high redshift (see figure 3). Very massive stars in the range 270-500 $M_\odot$

can play an important role for reionizing the IGM (see figure 3) as they add an intense ionizing flux without metal production. On the other hand the intensity of a starburst of PISN stars in the range 140-260 $M_\odot$ is strongly limited to avoid an overproduction of metals. Therefore such stars are not good candidates for the early reionization of the IGM (see figure 3). We conclude that intermediate minimum halo masses in the range $M_{\rm min} \sim 10^8 - 10^9$ $M_\odot$ and massive population III stars in the range 40-100 $M_\odot$ are preferred. This corresponds to an epoch of reionization at $z \sim 10-15$ in agreement with WMAP results (Kogut *et al.* (2003)). In such models, we predict that the early population III starburst is responsible for $\sim 10\%$ of metals in the IGM and that the observed cosmic SFR is underestimated above $z \sim 3$. It is interesting that the measurement of the type II SN rate at $z \sim 2-3$ should severely discriminate among the different possible minimum dark matter halo masses (see Figure 1 middle).

3. Supernovae

Once the intensity and the timescale of the normal mode of star formation have been fixed (see previous section), it is possible to constrain the parameters fixing the type Ia supernova rate. For type Ia progenitors in the mass range 2-8 $M_\odot$, we find that observations are well reproduced if ~ 1 % of these stars lead to type Ia supernovae and if the typical delay between the formation of the white dwarf and the explosion is $\sim 3-3.5$ Gyr (figure 4). This delay is much larger than what was usually assumed in the past (~ 1 Gyr), as already suggested by Dahlen *et al.* (2004). With such parameters, we predict that ~ 50 % of Iron in the structures is produce by type Ia supernovae (figure 2), whereas, due to the large delay, this fraction is only ~ 10 % in the IGM.

4. Conclusion

It is very promising that our model of cosmic evolution is able to reproduce simultanesouly a large set of independent observations at low and high redshift : present fraction of baryons in the star-forming structures, observed cosmic SFR, observed type II and type Ia supernovae rates, and chemical abundances in the structures and in the IGM. We predict that the bulk of the star formation occurs in collapsed structures having dark matter halos of minimum mass $10^8 - 10^9$ $M_\odot$, that the observed SFR above $z \sim 3$ is probably underestimated, that population III stars are mainly in the range 40-100 $M_\odot$, that only 10 % of the metals in the IGM are due to these populations III stars, that the reionization of the IGM occurs at $z \sim 10-15$ and is easier if population III stars also include a very massive component above 270 $M_\odot$, and that type Ia supernovae explode with a long delay $\sim 3-3.5$ Gyr and are therefore responsible of 50 % of Iron in the structures but only 10 % in the IGM.

Acknowledgements

F.D. and E.V. thanks K. Olive, P. Petitjean, J. Silk and F. Stoehr for permanent exciting discussions.

References

Aguirre, A., Schaye, J., Kim, T. *et al.* 2004, ApJ, 602, 38
Bessell, M. S., Christlieb, N. & Gustafsson, B. 2004, ApJ, 612, L61
Blanc, G., Afonso, C., Alard *et al.* 2004, A&A, 423, 881
Bromm, V. 2004, PASP, 116, 103

https://doi.org/10.1017/S1743921305005430 Published online by Cambridge University Press

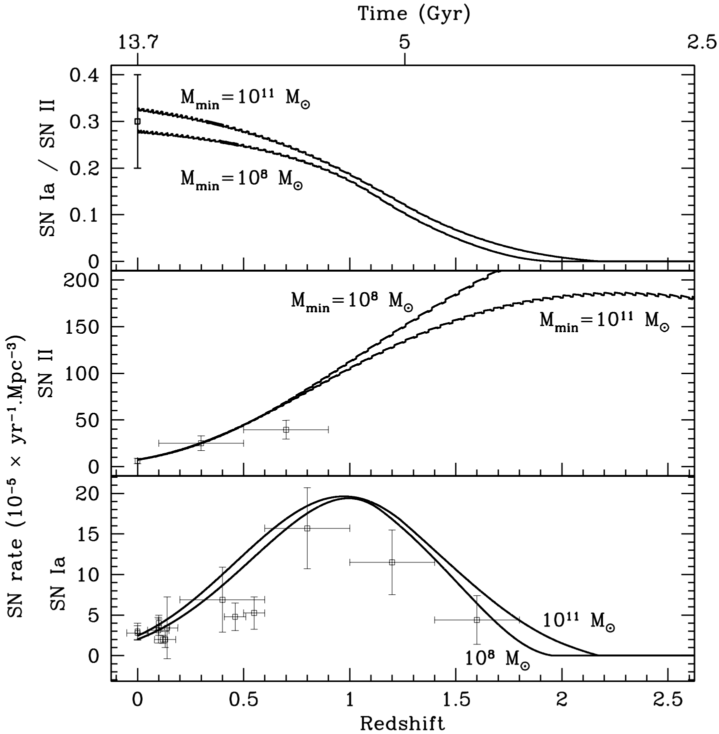

Figure 4. Evolution of the type Ia / type II Supernova rates. *Top : evolution of the ratio of type Ia over type II supernova event rates.* The observed local value is taken from Cappellaro *et al.* (1999). *Middle : type II SN rate as a function of redshift.* The observed rate up to $z \sim 0.7$ is taken from Dahlen *et al.* (2004). *Bottom : type Ia SN rate as a function of redshift.* The observed rate up to $z \sim 1.6$ is taken from Blanc *et al.* (2004), Dahlen *et al.* (2004) and Strolger *et al.* (2004). In the three panels, the result of two models with $M_{\rm min} = 10^8$ $M_\odot$ and $M_{\rm min} = 10^{11}$ $M_\odot$ is plotted in thick line. Models for $M_{\rm min} = 10^7$ and 10^9 $M_\odot$ are not plotted but are very close to the model with $M_{\rm min} = 10^8$ $M_\odot$.

Cappellaro, E., Evans, R. & Turatto, M. 1999, A&A, 351, 459
Daigne, F., Olive, K. A., Vangioni-Flam, E., Silk, J. & Audouze, J. 2004, ApJ, 617, 693
Daigne, F., Olive, K. A., Silk, J., Stoehr, F. & Vangioni-Flam, E. (2005) to be submitted
Depagne, E., Hill, V., Spite, M., Spite, F. *et al.* 2002, A&A, 390, 187
Dahlen, T., Strolger, L., Riess *et al.* 2004, ApJ, 613, 189
Frebel, A., Aoki, W., Christlieb, N. *et al.* 2005, Nature, 434, 871
Fukugita, M. & Peebles, P. J. E. 2004, ApJ, 616, 643
Hopkins, A. M. 2004, ApJ, 615, 209
Jenkins, A., Frenk, C. S., White, S. D. M. *et al.* 2001, MNRAS, 321, 372
Kogut, A., Spergel, D. N., Barnes, C. *et al.* 2003, ApJS, 148, 161
Ledoux, C., Petitjean, P. & Srianand, R. 2003, MNRAS, 346, 209
Plez, B. & Cohen, J. G. 2005, A&A, 434, 1117
Press, W. H. & Schechter, P. 1974, ApJ, 187, 425
Prochaska, J. X., Gawiser, E., Wolfe, A. M., Castro, S. & Djorgovski, S. G. 2003, ApJ, 595, L9
Songaila, A. 2001, ApJ, 561, L153
Spergel, D. N., Verde, L., Peiris, H. V. *et al.* 2003, ApJS, 148, 175
Strolger, L., Riess, A. G., Dahlen *et al.* 2004, ApJ, 613, 200
Tinsley, B. M. 1980, Fund. of Cosmic Phys., 5, 287

https://doi.org/10.1017/S1743921305005430 Published online by Cambridge University Press